Transactions in Optics and Photonics
http://ojs.wiserpub.com/index.php/TOP/

Research Article

Complexity in Nonlinear and Quantum Optics by Considering Kolmogorov Derivatives and Change Complexity Information Measures

Dragutin T. Mihailović

Department of Physics, Faculty of Sciences, University of Novi Sad Dositej Obradovic Sq. 3, Novi Sad, 21000, Serbia
Email: guto@df.uns.ac.rs

Received: 12 August 2024; **Revised:** 9 January 2025; **Accepted:** 14 January 2025

Abstract: One of the most challenging tasks in studying phenomena in nonlinear and quantum optics is determining the contributions of the complexities of individual components to the complexity of the entire system (master complexity). To examine these contributions, we considered this issue using information measures: Kolmogorov derivatives based on Kolmogorov complexity (KC) [KC spectrum, KC plane], change complexity (*CC*), and Lyapunov exponent (λ). We applied these measures to daily time series measured from 2003 to 2005 in Novi Sad (Serbia) for ultraviolet (UV) radiation, which represents a physical complex system, and water vapor pressure as individual components of that system. Based on the measures applied to UV radiation, we determined: (i) the level of chaos and randomness of the measured time series; (ii) the coordinates of points in the KC plane where master and individual amplitudes interact; and (iii) the range of UV radiation amplitudes in which changes in the interaction between the master and individual amplitudes are most pronounced.

***Keywords*:** nonlinear optics, UV radiation Kolmogorov complexity (KC), KC spectrum, KC plane, change complexity, lyapunov exponent

1. Introduction

Nonlinear and quantum optics is a complex physical system that deals with phenomena occurring when light interacts nonlinearly with materials. We have witnessed rapid growth in research in the fields of nonlinear and quantum optics, reflected in increased investment, applications, and publications [1-3]. This progress is evident across various platforms where nonlinear and quantum optics are considered, including space-time complexity, measurements, the creation of a new table listing nonlinear optical properties of materials, structured light, and information processing, among others [4-12].

This paper considers UV radiation as a type of physical complex system influenced by the surrounding environment. In general, and specifically in nonlinear and quantum optics, methods for obtaining information from complex systems can be divided into three categories: (1) analyzing data, (2) constructing and evaluating models, and (3) searching for information using various information measures. Point (1) is primarily addressed by traditional mathematical statistics. The use of heuristic models of varying levels of sophistication is widespread [13]. However, model designers encounter many obstacles, mainly due to (1) interlocked interactions between the components of a

DOI:

complex system and (2) the occurrence of additional information that originates from the system but is not visible to the observer. If we ignore these factors, an analysis of such a system becomes impossible. To our knowledge, this is perhaps the first application, in nonlinear and quantum optics, of a set of information measures: Kolmogorov complexity (KC), Kolmogorov complexity spectrum (KC spectrum), Kolmogorov complexity plane (KC plane) [14], change complexity (*CC*), and Lyapunov exponent (λ). These information measures were applied to daily time series of UV radiation and water vapor pressure measured in Novi Sad (Serbia) from 2003 to 2005 in the analysis of their chaos, randomness, and complexity. After the introductory part (Section 1), Section 2 contains the methodology and data used, while Section 3 is devoted to results and discussion. Concluding remarks are presented in Section 4.

2. Methodology: information measures and data used

Kolmogorov complexity. KC (Kolmogorov complexity) of a given object is defined as the size of the shortest program that generates an object. KC is the incomputable measure that is approximated by the Lempel-Ziv algorithm (LZA) [15] and its variants (see Appendix A [13]). This algorithm operates with binary time series depending on the choice of the threshold value.

Kolmogorov complexity spectra. If the above algorithm is applied N times to a time series $\{x_i\}$, using all elements of $\{x_i\}$ as thresholds $\{x_{tr,\,i}\}$ forming the time series $\{c_i\}$, $i = 1, 2, 3, \ldots, N$, then time series $\{c_i\}$ is the KC spectrum of a time series $\{x_i\}$. This series is transformed into binary strings by time a series of thresholds $\{x_{tr,\,i}\}$, $i = 1, 2, 3, \ldots, N$. By application of the LZA algorithm the original time series is converted into a set of 0-1 sequence $\{S_i^{(k)}\}$, $i = 1, 2, 3, \ldots, N$, $k = 1, 2, 3, \ldots, N$ defined by comparison with a threshold $x_{tr,\,k}$,

$$S_i^{(k)} = \begin{cases} 0 & x_i < x_{tr,\,k} \\ 1 & x_i \geq x_{tr,\,k} \end{cases}. \qquad (1)$$

After applying the LZA algorithm to each element of the series $\{S_i^{(k)}\}$, we get the KC spectrum $\{c_i\}$, $i = 1, 2, 3, \ldots, N$ [11].

The KC spectrum examines complex systems with high complexity. Figure 1 shows the KC spectra for quasi-periodic, Lorenz attractor, random with the constant distribution and random with the Poisson distribution time series. It is seen how is easy to discriminate chaotic and quasi-periodic curves from those of the random series.

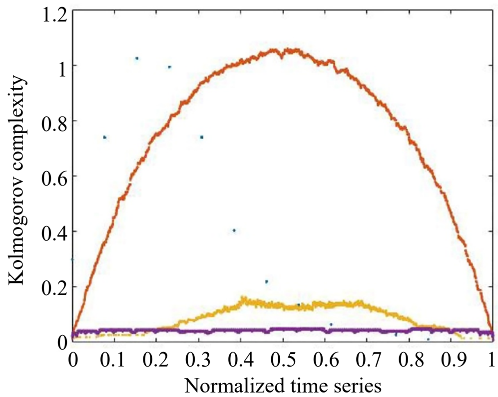

Figure 1. KC spectrum for different time series: (i) quasi-periodic (pink curve), (ii) Lorenz attractor (yellow curve), (iii) random with the constant distribution (orange curve), and (iv) random with the Poisson distribution (dots) [13] (Figure courtesy of Marcelo Kovalsky)

As mentioned, one of the most challenging tasks in studying complex physical systems is determining how the complexities of individual components contribute to the overall complexity of the system. Concerning this issue, Mihailović et al. [14] proposed the Kolmogorov complexity plane (KC plane), based on the KC spectrum. From the KC plane, it is possible to determine the intervals of interacting amplitudes: master (for the entire system) and individual (for components). It will be shortly demonstrated using time series $\{x_i\}$ obtained by the instrument $\{M_\varepsilon, \varepsilon\}$ with $\{M_\varepsilon, \varepsilon\} = e^{-w\sigma}$, where w is the amplitude factor, σ is the random number uniformly distributed in the interval [0, 1], and sampling $\tau = 1$. Here, the state space M_ε, consists of cells of size ε that are sampled at each time sample point τ, while the measured time series consists of the successive elements M_ε. Using the instrument $\{M_\varepsilon, \varepsilon\}$, we get information as a time series of states $\{x_i\}$.

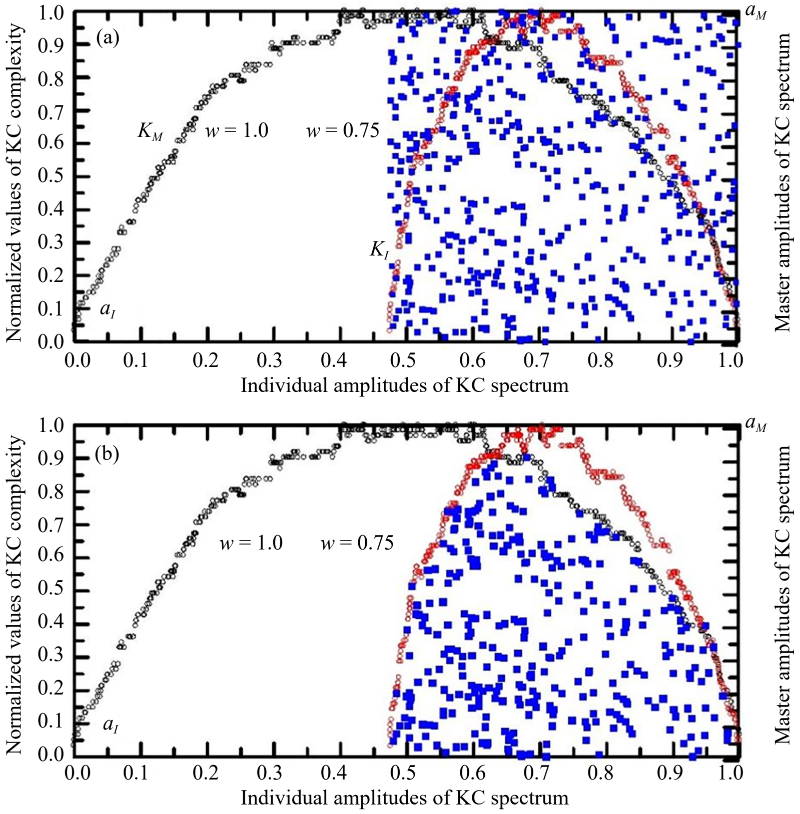

Figure 2. (a) The values of interacting amplitudes of the master and individual KC spectra set along a_M and a_I axes (blue squares), respectively. KC spectra of the entire system (K_M, black circles) and its component (K_I, red circles) were calculated from the time series generated by the instrument $\{M_\varepsilon, \varepsilon\} = e^{-w\sigma}$ for $w = 0.75$ and $w = 1.0$ (see previous subsection), (b) the same as in Figure 2a but with interacting amplitudes included in the set defined by Eq. (2) (blue squares)

A comparison of the two KC spectra is shown in Figure 2a, which represents two merged two-dimensional graphs (with different meanings of axes): (1) KC master vs. individual components (both amplitudes are on the x-axis and both complexities on the y-axis) and (2) a_M (the master amplitude) vs. a_I (individual amplitude), i.e., the KC plane. The black and red circles represent master (K_M) and individual spectra (K_I), which are calculated from the time series generated by the instrument $\{M_\varepsilon, \varepsilon\} = e^{-w\sigma}$ for $w = 0.75$ and $w = 1.0$. At the same time, the squares indicate points in the KC plane. The quantities in these two planes were compared in the two-dimensional system (0, 1) using normalized time series. Since these quantities are on the same scale after normalization, we can evaluate their relationships and patterns without the influence of varying scales [16]. Furthermore, Figure 2a shows that the squares in the (a_I, a_M) system are scattered. This is due to the dynamic relationship and interdependence between the “master” variant and individual ones. It can also be seen that there are two groups of points. One set belongs to the area under the K_M spectrum curve (denoted as S_m), while another belongs to the area under the K_I spectrum curve (denoted as S_i). However, only points from the set S_p defined as

$$S_p = S_m \cap S_i \tag{2}$$

are the candidates suitable for comparing the complexity of different sequences or systems (in this case, the entire complex physical system and its components). The amplitudes that belong to this set will conditionally be called *interactive amplitudes* (Figure 2a).

What should we do to derive a conclusion about the relationship between interacting amplitudes in the overlapping area of the two Kolmogorov complexity spectra in the KC plane?

We should choose a method to analyze overlapping complexity spectra. In this paper, we employ the so-called *change complexity*. This complexity appears to be suitable for analyzing the overlapping regions in the spectra, revealing the presence of nonlinearities in detecting UV radiation by pyranometers.

Change complexity. The concept of change complexity is relatively new in science in the analysis of binary time series, and at its core, unlike other informational measures, is based on change. Change aids an intuitive understanding of processes and is a measurable metric. Its origins stem from research in psychology, where quantification through short strings is of great importance. However, it is slowly but surely carving out its niche in other sciences, particularly in physics. Change complexity (*CC*) of a binary string *S* is

$$CC = \sum_{i=2}^{L} p_i w_i, \quad w_i = \frac{1}{L-i+1}, \tag{3}$$

where p_i, $i = 2, \ldots, L$ are elements of the array $P = (p_2, p_3, \ldots, p_L)$ called change profile of the string S, w_i, $i = 2, \ldots, L$ are weights, and L is the length of the string S. More formal mathematical descriptions and definitions of change profiles and weights are available in [13].

Data used. The measurements of UV radiation are recorded by the abroad band YankeeUV-B1biometer [17] placed at the area of the University of NoviSad (45.33° N, 19.85° E, and 84 m a.s.l.). It detects UV radiation every 30 seconds, while the data recording time was over 10-minute intervals from 2003 to 2005. Technical details, maintenance, and history of its calibration as well as other details are available in Malinović-Milićević et al. [18]. The daily data of water vapor pressure, for the period 2003-2005, were taken from the nearest meteorological station Rimski Šancevi included in the meteorological network of the Republic Hydrometeorological Service of Serbia. The station is located 8.5 km from the instrument location. The daily time series of both quantities are given in Figure 3.

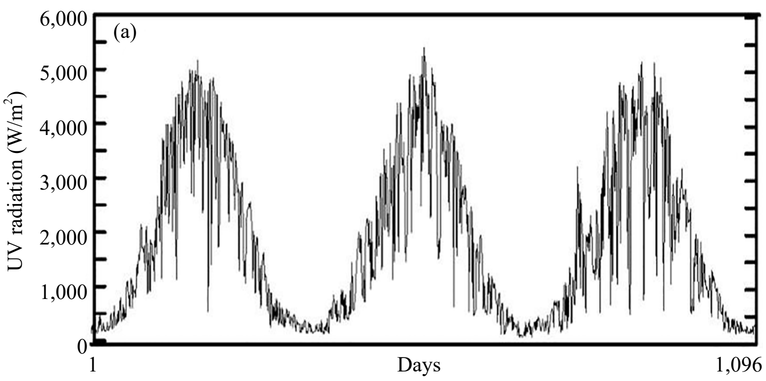

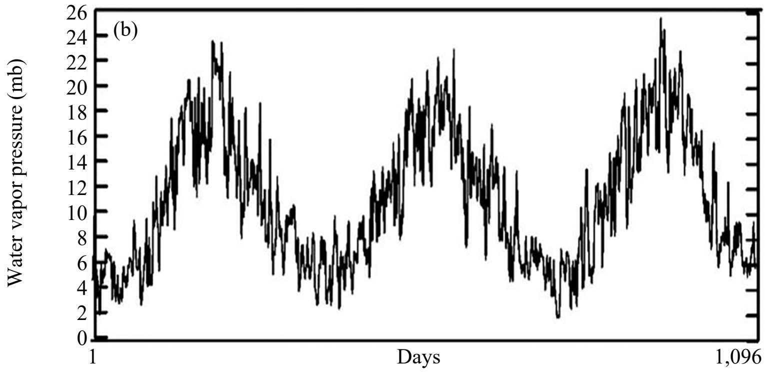

Figure 3. Daily time series of (a) the UV radiation and (b) water vapor pressure in Novi Sad (Serbia). The UV radiation was measured by the Yankee UV-B1 biometer during the period 2003-2005

3. Results and discussion

The measurement of UV radiation is a complex physical system *par excellence*. It encompasses various methods and technologies that require proper calibration and an understanding of the fundamental principles of optics, which are continuously evolving. Significant atmospheric factors influencing UV radiation include cloud cover, aerosols, ozone, temperature, and humidity. Notably, the complexity of UV radiation and humidity are inversely related; higher humidity tends to reduce the complexity in the UV radiation time series.

We first analyze the relationship between UV radiation and humidity (measured through water vapor pressure) using KC spectrum analysis (a quantitative tool for assessing and comparing the complexity of these two variables over time) and the KC plane.

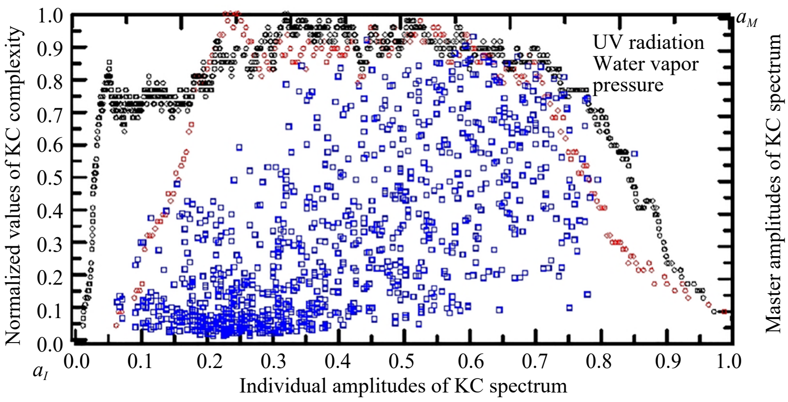

Figure 4. KC spectra of UV radiation (black empty circles) and water vapor pressure (red empty circles). a_M and a_I axes (blue empty squares) in the KC plane, respectively. Daily values of UV radiation for Novi Sad (45° 15’ N, 19° 50’ E) were obtained from measurements recorded by a broadband Yankee UV-B1 biometer during the period from 2003 to 2005. Daily data on water vapor pressure for the same period were taken from the nearest meteorological station, Rimski Šancevi, which is part of the meteorological network of the Republic Hydrometeorological Service of Serbia and located 8.5 km from the instrument

In our analysis of daily time series, we use UV radiation (the master amplitude) and water vapor pressure (the individual amplitude) data for Novi Sad, Serbia. The time series consists of $\boldsymbol{N}$ = 1,096 observations, with the highest values recorded at 5,394 W·m^{-2} for UV radiation and 25.3 mb for water vapor pressure Figure 4 depicts the KC spectra of UV radiation (black circles) and water vapor pressure (red circles), along with points in the KC plane (blue squares). There are 963 points located in the area beneath both spectra and 133 points outside this area. To assess the level of randomness and chaotic behavior in these time series, we calculated the KC and Lyapunov exponent ($\boldsymbol{\lambda}$) using the method proposed by Rosenstein et al. [19]. The time series exhibits low chaos (with $0.025 \leq \boldsymbol{\lambda} \leq 0.080$) and randomness (with $0.440 \leq KC \leq 0.583$), which is characteristic of UV radiation time series. It is important to note that the terms "random" and "chaotic" are often used synonymously, despite their distinct meanings. Randomness indicates disorder with a complete absence of patterns, while chaotic systems possess an underlying order or pattern despite apparent disorder.

Examining the distribution of points in this area within the individual amplitude interval (0, 0.4), we observe that the complexities are relatively low (ranging from 0 to 0.3). What quantitative conclusions can we draw from the data presented in Figure 4? We can only state that the influence of interactive water vapor amplitudes on UV radiation complexity is observed (1) throughout the range of these amplitudes and (2) within a narrow complexity interval (0, 0.4). Moreover, these findings appear to provide a solution to the question of how humidity, as part of a physical complex system (the measurement of UV radiation), affects its overall complexity. Let us note that if the KC spectra of the time series partially overlap, it could indicate that there are similarities or patterns present in the data at different levels of complexity. This suggests that certain aspects of the data maintain a consistent level of complexity across different scales or resolutions. There are several possible interpretations of partially overlapping KC spectra for two or more time series, including shared patterns, similar complexity profiles, overlapping generative mechanisms, and non-random similarities. Potential applications of this concept include time series clustering, anomaly detection, and feature extraction.

In this paper, we analyze the region of the partially overlapping spectra using change complexity. Change complexity is a computable measure that quantifies the complexity of a sequence or pattern based on the number of changes between its elements. It is particularly sensitive to regularities such as symmetries and periodicities. Originally used for the analysis of short strings in psychology, it has also demonstrated advantages in other disciplines, particularly in physics.

First, we create a quadratic matrix $\boldsymbol{A}$ (4) defined as $[A_{i,j}]$ where $i, j = 1, 2, 3, \ldots, N$. The elements of this matrix represent the numbers of interactive amplitudes in the (a_I, a_M) system shown in Figure 4.

$$A = \begin{bmatrix} 0 & 0 & 0 & 0 & 1 & 1 & 0 & 0 & 0 & 0 \\ 0 & 0 & 0 & 2 & 3 & 12 & 13 & 1 & 0 & 0 \\ 0 & 0 & 0 & 6 & 10 & 19 & 12 & 3 & 0 & 0 \\ 0 & 0 & 0 & 5 & 14 & 17 & 26 & 3 & 0 & 0 \\ 0 & 0 & 3 & 9 & 13 & 12 & 16 & 6 & 0 & 0 \\ 0 & 4 & 6 & 16 & 16 & 15 & 14 & 12 & 0 & 0 \\ 0 & 12 & 11 & 17 & 26 & 18 & 11 & 7 & 0 & 0 \\ 3 & 4 & 13 & 25 & 25 & 13 & 7 & 6 & 0 & 0 \\ 0 & 29 & 45 & 43 & 16 & 214 & 4 & 2 & 0 & 0 \\ 3 & 78 & 153 & 60 & 15 & 9 & 1 & 1 & 0 & 0 \end{bmatrix}. \tag{4}$$

Rows (i) correspond to individuals, while columns (j) represent master interactive amplitudes. N is the number of intervals of interactive amplitudes in this system (in this paper, we set $\boldsymbol{N} = 10$). Each type of matrix $\boldsymbol{A}$ indicates how many individual amplitudes interact with the master amplitude in a given interval. We refer to the string formed from such a sequence of numbers as the individual string, denoted as $\mathbb{S}_I$. Additionally, we define a string whose elements are the sums of the numbers in each row of the master string ($\mathbb{S}_M$).

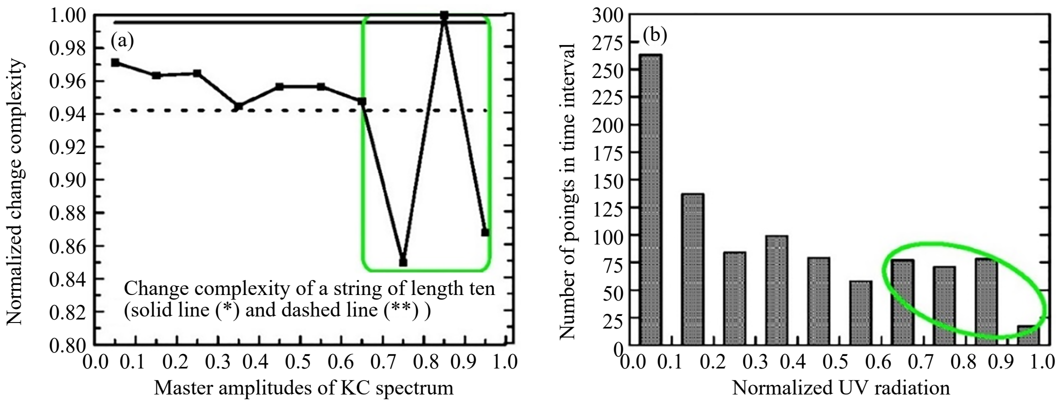

Figure 5. (a) Change in complexity (*CC*) of (i) the master string $\mathbb{S}_M$ (*), (ii) the variation of individual strings, and the mean value of change complexity of individual strings $\mathbb{S}_I$ (**); (b) dependence of the number of points in a time interval on UV radiation in the time series shown in Figure 3

In Figure 5a, the change complexity of the master string $\mathbb{S}_M$ has a value close to one (which is the highest possible value for change complexity). Therefore, the *CC* complexity calculated in this way indicates a high level of interaction complexity between the master and individual amplitudes in the KC plane, ignoring differences from interval to interval. These differences are not dominant. However, after interval 0.6, abrupt changes occur, characterized by two drops and one jump in complexity. In other words, this passage states that after an interval of 0.6, the complexity exhibits a pattern of two decreases followed by one increase, resulting in an unforeseen change in the complexity profile within that interval (indicated by the green rounded rectangle). Figure 5b further explains this behavior of change complexity. In the area bounded by the green ellipse, at high amplitudes of UV radiation, the changes in the interaction between the master and individual interactive amplitudes are most pronounced.

4. Conclusions

(1) Considering the impact of the complexity of humidity on the entire complexity of UV radiation measurements, we realized this through the following steps: (i) selection of two time series encompassing the daily measurements of UV radiation taken by the broadband Yankee UV-B1 biometer and the daily measurements of water vapor pressure for the period 2003-2005 in Novi Sad, Serbia; (ii) computing the information measures Kolmogorov complexity (KC), Kolmogorov complexity spectrum (KC spectrum), and coordinates of points in the Kolmogorov complexity plane (KC plane); (iii) creating a quadratic matrix whose elements represent the numbers of interactive amplitudes (master and individual), Lyapunov exponent (λ), and change complexity (*CC*) for both time series.

(2) (i) The time series exhibit low chaos (with $0.025 \leq \lambda \leq 0.080$) and randomness (with $0.440 \leq \text{KC} \leq 0.583$), which is characteristic of UV radiation time series. (ii) The KC spectra of both time series highly overlap, indicating that there are similarities or patterns present in the data at different levels of complexity (from N = 1,096 observations, there are 963 points located in the area beneath both spectra and 133 points outside this area). (iii) The calculated *CC* complexity indicates a high level of interaction between the master and individual amplitudes in the KC plane, ignoring differences from interval to interval. (iv) At high amplitudes of UV radiation, changes in the interaction between the master and individual amplitudes are most pronounced.

(3) The use of KC spectra, KC plane, and change complexity provides powerful tools for analyzing complex systems in optics and photonics, with diverse applications ranging from environmental monitoring to advanced sensor development, modeling of nonlinear optical phenomena, and feature extraction for machine learning.

Acknowledgements

I thank Mi. Anja Mihailović for useful comments and assistance in the computing part of the work.

Conflict of interest

The author declares no competing financial interest.

References

[1] Ren M, Xu JJ, Lan PF, Lu PX, Li ZY, Li HH, et al. Roadmap on nonlinear optics-focus on Chinese research. *Journal of Physics: Photonics*. 2023; 5(3): 032501.

[2] Ji WY, Jin C, Xu HX, Gao JR, Gröblacher S, Urbach P, et al. Recent advances in metasurface design and quantum optics applications with machine learning, physics-informed neural networks, and topology optimization methods. *Light: Science and Applications*. 2023; 12 (1): 169.

[3] Elliot M, Oscar S, Kathryn M. Current quantum optics research: Exploring the potential of quantum computing. *Journal of Tecnologia Quantica*. 2024; 1(1): 30-39.

[4] Arecchi FT. Space-time complexity in nonlinear optics. *Physica D*. 1991; 51(1-3): 450-464.

[5] Smolorz S, Wise F, Borelli NF. Measurement of the nonlinear optical response of optical fiber materials by use of spectrally resolved two-beam coupling. *Optics Letters*. 1999; 24(16): 1103-1105.

[6] Vermeulen N, Espinosa D, Ball A, Ballato J, Boucaud P, Boudebs G, et al. Post-2,000 nonlinear optical materials and measurements: Data tables and best practices. *Journal of Physics: Photonics.* 2023; 5(3): 032501.

[7] Buono WT, Forbes A. Nonlinear optics with structured light. *Opto-Electron Advances*. 2022; 5(6): 210174.

[8] Caterina EM, Briegel HJ, Kraus B. Quantum Kolmogorov complexity and its applications. *International Journal of Quantum Information*. 2007; 5(5): 729-750.

[9] Epstein S. *An Introduction to Algorithmic Information Theory and Quantum Mechanics*. France: HAL Science Ouverte; 2023. Available from: https://hal.science/hal-04072076v2/document [Accessed 20th January 2024].

[10] Rizvi STR, Seadawy AR, Mustafa B. Discussion on chirped periodic and optical soliton solutions for chiral nonlinear Schrödinger dynamical equation with Bohm potential. *Optical Quantum Electronics*. 2024; 56(5): 768.

[11] Rizvi STR, Mustafa B. Optical soliton and bifurcation phenomena in CNLSE-BP through the CDSPM with sensitivity analysis. *Optical and Quantum Electronics.* 2024; 56(3): 393.

[12] Rizvi STR, Mustafa B, Abbas SO. Generation of optical dromions to generalized stochastic nonlinear Schrödinger equation with Kerr effect and higher order nonlinearity. *Chinese Journal of Physics*. 2024; 91: 183-198. Available from: https://doi.org/10.1016/j.cjph.2024.07.003.

[13] Mihailović D, Kapor D, Crvenković S, Mihailović A. *Physics of Complex Systems: Discovery in the Age of Gödel*. Boca Raton: CRC Press; 2023.

[14] Mihailović D, Singh V. Information in complex physical systems: Kolmogorov complexity plane of interacting amplitudes. *Physics of Complex Systems.* 2024; 5(3): 146-153.

[15] Lempel A, Ziv J. On the complexity of finite sequences. *IEEE Transactions on Information Theory.* 1976; 22(1): 75-81.

[16] Asesh A. Normalization and bias in time series data. In: Biele C, Kacprzyk J, Kopeć W, Owsiński JW, Romanowski A, Sikorski M. (eds.) *Digital Interaction and Machine Intelligence*. Switzerland: Springer; 2021. p.88-87.

[17] Yankee Environmental Systems, Inc. *UVB-1 UV Pyranometer, Installation and User Guide, 2000, version 2.0*. Turners Falls, MA, USA: Yankee Environmental Systems, Inc; 2000.

[18] Malinović-Milićević S, Mihailović A, Mihailović DT. Kolmogorov complexity analysis and prediction horizon of the daily erythemal dose time series. *Atmosphere.* 2022; 13(5): 746-762.

[19] Rosenstein MT, Collins JJ, De Luca CJ. A practical method for calculating largest Lyapunov exponents from small data sets. *Physica D*. 1993; 65(1-2): 117-134.